ADVANCES IN GEODESY AND GEOINFORMATION
(formerly GEODESY AND CARTOGRAPHY)
Vol. 73, no. 1, article no. e50, 2024

https://doi.org/10.24425/agg.2023.146162

Original paper

The Nova Kakhovka dam collapse flooding as seen from Sentinel-1 SAR satellite images

Roberto Monti*, Lorenzo Rossi, Mirko Reguzzoni

Politecnico di Milano, Milan, Italy
e-mail: roberto.monti@polimi.it; ORCID: http://orcid.org/0009-0006-1608-6648
e-mail: lorenzo1.rossi@polimi.it; ORCID: http://orcid.org/0000-0001-6050-1972
e-mail: mirko.reguzzoni@polimi.it; ORCID: http://orcid.org/0000-0002-4027-9347

*Corresponding author: Roberto Monti, e-mail: roberto.monti@polimi.it

Received: 2023-10-18 / Accepted: 2024-04-12

Abstract: The destruction of the Nova Kakhovka dam in Ukraine on June 6th, 2023, produced an enormous flooding in the entire Kherson region. Thousands of people and agricultural fields were affected, bringing down an economy already devastated by the ongoing war. In addition to that, in the months prior to the collapse, the water level in the reservoir has been firstly decreased to a minimum, before rising it to an all-time maximum. Both these two situations are studied by means of Sentinel-1 SAR images, using the so-called change detection technique, with the aim of identifying those areas that got covered by water due to the Lake Kakhovka level rise and due to the flooding in the downstream region of the dam. The obtained results are then validated through comparison with optical images from Sentinel-2 and Landsat 9 satellites. The initial validation involves a visual assessment of both data types, followed by a more in-depth analysis that includes pixel classification of the optical images. This final step enables a precise quantification and comparison of the extent of the damage. It is clear that the increase of the water level before the dam collapse has worsened the extension and effect of the subsequent flooding.

Keywords: SAR, Sentinel-1, Change detection, Remote sensing, Nova Kakhovka dam

1. Introduction

The Nova Kakhovka Dam (Finnis, 2023), also known as Dniprohes, was a dam located on the Dnieper River in Ukraine. It was one of the largest hydroelectric dams in Europe and was situated near the city of Nova Kakhovka in the Kherson region. The dam was built between 1950 and 1956, with the goals of producing hydroelectric power, controlling the flow of the Dnieper River, and storing water for irrigation of nearby agricultural lands. The

dam was roughly 61 m tall and 1.5 km long. One of the biggest artificial lakes in Ukraine, Lake Kakhovka, was its reservoir, which had a surface area of about 2,155 km^2. With its contributions in electricity production, control of the Dnieper River's flow for navigation and irrigation, and provision of recreational opportunities for locals and visitors, the Nova Kakhovka Dam and its hydroelectric power plant had a significant and positive impact on the local economy and agriculture (Hoybye et al., 2002).

In the aftermath of the Russian Federation's invasion of Ukraine in February 2022, the southern bank of the river, including the Nova Kakhovka dam and the Zaporizhzhia nuclear power plant, came under the control of the occupiers (Yerushalmy, 2023). Despite the occupation, the production of hydroelectric power from the dam reservoir continued working without significant alterations until a peculiar event occurred in January 2023. During this time, there was an unexpected drop in the water level of the reservoir, reducing it by more than two meters from the average. The exact cause of this decline is uncertain and would require more detailed information. However, it is important to note that factors such as changes in water management, altered river flow patterns, or deliberate actions by the occupying forces could have contributed to this event. Subsequently, the water level began to rise again, reaching an all-time high in the first days of June 2023 (USDA Foreign Agricultural Service, 2023). Again, without access to more detailed and accurate information, it is challenging to make definitive conclusions about the underlying reasons for the rise in water level.

On June 6th, 2023, an underwater explosion destroyed part of the vertical facing of the dam, with the subsequent flooding of both banks of the Dnieper River, affecting agricultural fields as well as villages (and even the southern part of the city of Kherson), up to the Black Sea (Vyshnevskyi et al., 2023). It has been defined as one of the biggest industrial and ecological disasters in Europe for decades (Kottasova and Mezzofiore, 2023). This catastrophe destroyed entire villages, flooded farmland, deprived tens of thousands of people of power and clean water and caused massive environmental damage (Gleick et al., 2023; Knight, 2023; Kuzova, 2023).

In emergency situations, real-time access to accurate and reliable data is crucial for assessing the magnitude of a disaster and effectively coordinating the initial response efforts. Timely information allows emergency responders to understand the scope of the situation, prioritize their actions, and allocate resources effectively (Krichen et al., 2024). In such scenarios, freely available real-time data can play a vital role. These data can include information from various sources, such as satellite imagery (Smith and Butterworth, 2023), remote sensors, social media, and other data streams (Columb et al., 2003; Blum et al., 2013). These sources can provide valuable insights into the extent of the disaster, including the affected areas, population density, infrastructure damage, and potential hazards (Bullock et al., 2013; Reguzzoni et al., 2022). However, it is essential to verify and validate the obtained information, particularly in conflict zones or areas where on-site verification may be limited or even impossible due to safety concerns. Cross-referencing and triangulating data from multiple sources can help to check accuracy and improve situational awareness (Skarpa et al., 2023).

The Copernicus program (European Space Agency (2023b)), funded by the European Union (EU), is an invaluable resource for reliable and freely available Earth observation data. The program aims at providing accurate and up-to-date information for a variety of applications, including environmental monitoring, climate change analysis, emergency

management, and more. One of the main components of the Copernicus program is the Sentinel constellation of satellites. These satellites provide a wealth of data that are freely available to users around the world. The data cover land, atmosphere, sea, climate, and other domains. Sentinel data can be used in disaster management, environmental monitoring, urban planning, agriculture, and many other applications (DeVries et al., 2020; Malmgren-Hansen et al., 2020; Mitraka et al., 2020; Bitek and Erenoğlu, 2022; Tarpanelli et al., 2022). Access to reliable and free data through Copernicus greatly facilitates the work of researchers, policy makers and practitioners in various fields. It enables evidence-based decision-making, improves our understanding of Earth systems, and supports efforts to address a variety of global challenges (Mateo-Garcia et al., 2021; Apicella et al., 2022; Vavassori et al., 2022).

This work aims at investigating the repercussions associated with the destruction of the Nova Kakhovka dam. The primary objective of the proposed technique is to deliver a prompt and initial assessment of the flooding through rapid mapping techniques, using the first available satellite data. Specifically, a comparison of outcomes from optical and radar imagery will be conducted to comprehensively analyze the extent of the dam destruction. Additionally, any abnormal behaviors detected in the months leading up to the dam destruction will be explored. Therefore, this research contributes to a better understanding of the event and provides valuable insights for future preventive measures. This approach addresses not only the immediate impact of the dam destruction but also the methodological and technical aspects of remote sensing in disaster analysis. The paper is organized as follows: Section 2 provides an explanation of the satellite data used and the processing strategy employed. The outcomes of the conducted analysis are detailed in the "Results" section. Subsequently, in Section 4, a comparative analysis between radar and optical results is presented, encompassing both qualitative and quantitative assessments. The paper concludes with a summary of findings, as well as future perspectives.

2. Data used and methods applied

Sentinel images can be used to assess the extent of damage caused by natural disasters such as floods, earthquakes, fires, or storms. By comparing images before and after the disaster, analysts can identify changes in land cover, damage to infrastructure and the overall impact on affected regions. Sentinel-1 radar imagery (Torres et al., 2012) plays a crucial role in disaster management, providing timely and accurate information for monitoring and response efforts. Its abilities to penetrate clouds, to operate in both day and night, and to provide detailed information on surface characteristics make it a valuable asset for various applications in Earth observation and environmental monitoring. The Sentinel-1 satellite program (Fletcher, 2012), which, after the retirement of Sentinel-1B (European Space Agency, 2022a), includes the Sentinel-1A satellite only, provides significant global coverage for monitoring and observing places all over the world. It operates in a near-polar orbit and collects data from the whole Earth. This extensive coverage allows for monitoring of both land and maritime areas. Sentinel-1A provides frequent revisits to specific locations, offering continuous monitoring and the collection of time-series data. The precise revisit time is determined on the basis of the imaging mode and latitude of the target area. More generally, a location can be revisited as often as every twelve days.

Sentinel-1 carries a Synthetic Aperture Radar (SAR) instrument (Flores et al., 2019) that uses microwave frequencies to capture images of the Earth's surface. SAR systems work as follows: the radar sends pulses of microwave signals from the satellite antenna toward the Earth's surface. When the transmitted signal reaches the ground, it interacts with objects such as buildings, vegetation, and terrain. The signal is partially reflected to the radar system and partially scattered in all the other directions. SAR systems measure the intensity of the reflected signal, as well as the time it takes to travel to the target and back, thereby determining the range (or distance) to any point on the surface of the planet. By combining measurements of multiple radar pulses along a satellite flight path (also known as orbit), the instrument creates a larger virtual antenna aperture through synthetic aperture processing. The obtained image represents radar backscatter, which reflects the properties of the illuminated objects. SAR images can be then analyzed to extract information about land cover, surface roughness, vegetation, water bodies and man-made structures. This technology offers benefits such as all-weather and day-night imaging capabilities, as it can penetrate clouds, smoke, and foliage, making it invaluable for a variety of applications (Vincent, 2003).

Flood mapping using Sentinel-1 SAR data is based on the so-called change detection technique (Rignot and van Zyl, 1993), which compares pre- and post-flood radar images to identify and delineate the extent of the flooded areas (Stelmaszczuk-Gorska, 2020; Tay et al., 2020). First, the acquired SAR images undergo pre-processing steps to correct for radiometric and geometric distortions. These steps involve calibration, speckle filtering to reduce noise, and orthorectification, by the so-called terrain correction employing an available digital elevation model, e.g., the Copernicus one (European Space Agency and Airbus, 2022), to account for the Earth topography. Then, the two pre-processed images are geometrically aligned (coregistered) by means of a cross-correlation algorithm to ensure accurate pixel-to-pixel correspondence between them. This coregistration process compensates for any geometrical differences that may arise due to variations in sensor positioning or platform motion. The entire workflow was performed within SNAP (SeNtinel Application Platform) software (European Space Agency, 2023a), freely distributed by European Space Agency (ESA). Finally, the backscattered radar signal intensity before and after the crisis event is straightforwardly compared; regions exhibiting significant changes are indicative of flooded areas. To improve the readability of these data, a flood extent map is produced, highlighting the affected areas by using a false-color representation. More generally, the change detection technique can be also applied to investigate the presence or absence of water coverage on dry land, as in the case of the variation of the water level in a lake (Nasirzadehdizaji et al., 2019). So, using Sentinel-1 SAR data, an analysis for both the water level change in the reservoir and the flooding due to the collapse of the dam is here presented. For the study, the Ground Range Detected (GRD) products (European Space Agency, 2022b) are used. These products are images derived from the raw SAR data after radiometric and geometric distortions corrections. The vertical-to-vertical (VV) polarization is chosen because of its suitability in detecting changes in water surfaces. For the considered case study of Nova Kakhovka dam, a ground range image corresponding to a reference condition (low water level and not collapsed dam) and another one during the crisis scenario (high water level and collapsed dam) are selected. The chosen image epochs are reported in Table 1.

Table 1. Dates and resolutions of the used Sentinel-1A images. The pixel size refers to the processing resolution, while the acquisition one is 10 × 10 m for both events

Event	Reference	Crisis	Pixel size
Flooding	28/05/2023	09/06/2023	30 × 30 m
Water level change	28/05/2023	09/02/2023	10 × 10 m

When analyzing the flooding, it is important to note that the affected area is quite large. A possibility to reduce the computational burden when analyzing the flooding extent is to further process the SAR images with the so-called multi-looking technique (Vavriv and Bezvesilniy, 2013), averaging the radar data over a window of 3 pixels × 3 pixels to reduce the effects of speckle noise. The SNAP built-in operator (Braun, 2018) was used for this purpose, although alternative filtering methods (Mansourpour and Blais, 2006; Santoso et al., 2016; Yu et al., 2018) could be applied. However, given the expansive nature of the scenarios considered in this study, the chosen method proves satisfactory, as it will be shown in following Sections. Despite this, it is essential to recognize that the multi-looking process sacrifices the spatial resolution of the images, resulting in a coarser representation of the features on the ground, which is not a good option when analyzing the water level change. This is because variations in the coastal shape and the water level require a more detailed view to accurately assess them. Therefore, the images used for studying water level change may not undergo the multi-looking process, ensuring a higher resolution that captures the necessary details at the expense of the computational burden. In fact, maintaining a higher resolution for water level scenarios ensures that subtle changes in the coastal shape and water levels can be detected and analyzed effectively. As for the flooded area analysis, priority was given to the reduction of the speckle noise applying the multi-looking processing technique and allowing for a smoother representation of the affected areas, while reducing the computational burden.

Finally, to validate the accuracy and reliability of the obtained maps, a comparison with optical images will be presented. This validation process involved coregistration and comparison of the SAR-derived maps with medium-resolution optical images. There will be conducted two distinct comparisons: one qualitative and one quantitative. The qualitative assessment involves a visual comparison between radar and optical images, facilitating a quick evaluation of results over specific areas of interest. On the quantitative side, a numerical comparison between the datasets is performed through pixel classification. The optical images were imported into ArcGIS Pro where a classification algorithm was used to identify water areas and other relevant features. Following a meticulous selection of training samples for each class, the Support Vector Machine (SVM) algorithm (Kecman, 2005) was performed. SVM provides strong classification and regression capabilities for a wide range of applications, from text and image classification to predictive modeling, by determining the ideal hyperplane that maximizes the margin between various classes. This global optimization property can lead to a better generalization (the ability of a model to perform well on unseen or new data, beyond the ones it was trained on), even when dealing with a small number of classes, as in the analyzed scenarios.

3. Results

To ensure clarity and organization, the results pertaining to the flooding event and water level monitoring scenario are presented below, in two separate subsections. This approach allows for focused interpretation and a comprehensive understanding of the observed changes in each specific case. In both cases, the wet areas during the crisis situation are visually represented by using the red color. This is achieved by creating a false-color RGB image, where the pre-event image is assigned to the red channel, while the post-event one is assigned to the blue and green channels.

3.1. Water level monitoring

High-resolution SAR images were employed to monitor variations in the coastal shape and water level. The finer spatial resolution captured the intricacies of the coastal morphology, enabling accurate assessment of changes caused by fluctuations in water level. This first analysis focuses on the entire lake Kakhovka, encompassing its full extent. This comprehensive approach allows for a holistic assessment of the lake conditions and provides insights into the overall dynamics and changes occurring within the water body.

In Figure 1, areas of particular interest (AOI) are identified and highlighted in yellow. These AOIs represent specific locations or regions within the lake that have caught the attention for further investigations, to gain deeper insights into the observed water level variations and their potential implications. In addition to the SAR false-color image depicting the water level variation of lake Kakhovka, a comparison between the two epochs is provided for each identified AOI. This comparison is conducted using Sentinel-2 optical images. For accurate analysis and visualization, the selected Sentinel-2 images correspond as closely as possible to the dates of the SAR images, ensuring temporal consistency. By aligning the dates, it becomes easier to establish a direct comparison between the two conditions, facilitating the identification of changes and assessing their magnitude. The Sentinel-2 images used for this comparison are carefully chosen to have minimal or no cloud cover over the identified AOIs.

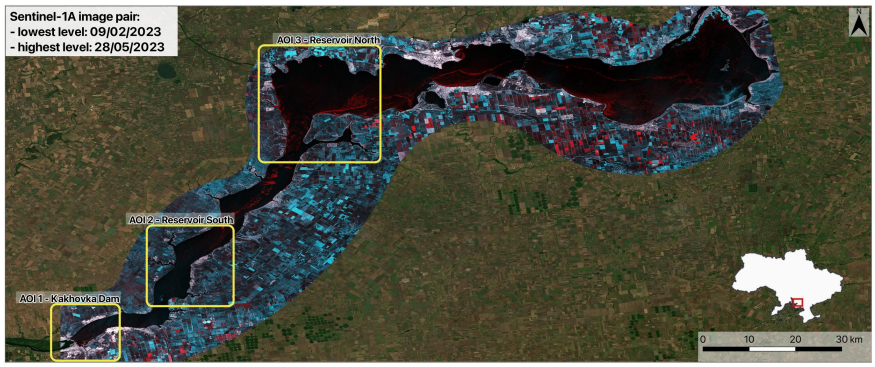

Fig. 1. SAR false-color image depicting the lake Kakhovka water level variation (see red pixels on the lake boundaries) between February 9th, 2023, and May 28th, 2023. Yellow borders identify some areas of interest (AOI), where additional studies are performed. A subset of the entire SAR image was created around the lake, only for computer memory issues

The first area of interest is the dam and its surrounding neighborhood. The increase in water level following the February reduction led to the submergence of the sandy coasts (Fig. 2c) that were previously visible (Fig. 2b). This change is a direct consequence of the altered hydrological conditions, where the water level has encroached upon and covered the sandy areas exposed in February.

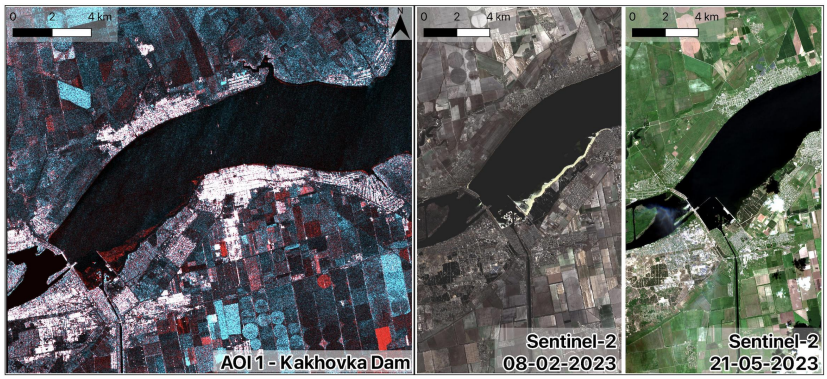

(a) (b) (c)

Fig. 2. Area of interest 1: Kakhovka dam. (a) SAR false-color image; (b) Sentinel-2 optical image, low water level situation; (c) Sentinel-2 optical image, high water level situation

The second AOI that is considered corresponds to the southern part of the reservoir, where few rivers disentangle themselves from the shores of the lake. Similar as before, the coastline appears in red, indicating the variation of the water level. This observation is consistent with the findings from the optical images, as shown in Figure 3.

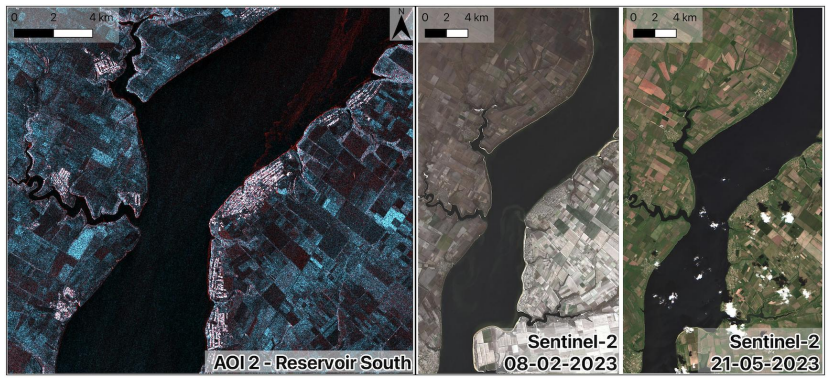

(a) (b) (c)

Fig. 3. Area of interest 2: Reservoir south. (a) SAR false-color image; (b) Sentinel-2 optical image, low water level situation; (c) Sentinel-2 optical image, high water level situation

Figure 4 shows the third, and last, AOI, which refers to the northern portion of the lake, where a bend is present. In this specific AOI, the exposure of the coastline is even more evident, both in the SAR and optical images.

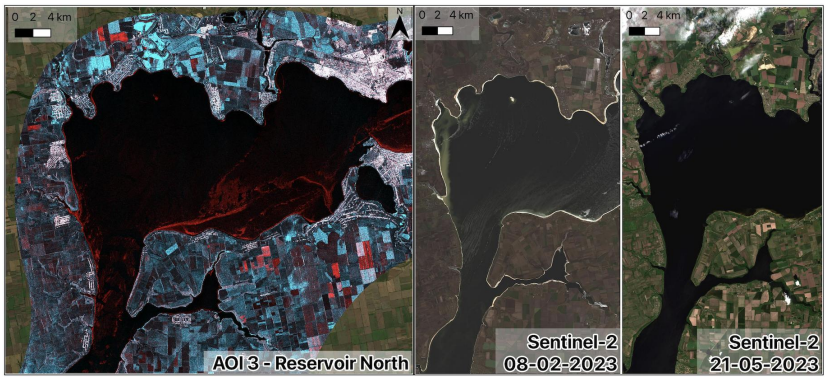

(a) (b) (c)

Fig. 4. Area of interest 3: Reservoir north. (a) SAR false-color image; (b) Sentinel-2 optical image, low water level situation; (c) Sentinel-2 optical image, high water level situation

3.2. Flooding

By utilizing multi-looked SAR images with reduced speckle noise, the extent of the flooded area was determined. The coarser resolution facilitated a smoother representation of the flooded regions, allowing for a comprehensive assessment of the flood extent. A straightforward comparison of pre- and post-flood images revealed significant changes in land cover within the affected area. These changes included the emergence of new water bodies, alterations in vegetation patterns, and potential damage to infrastructure (Fig. 5).

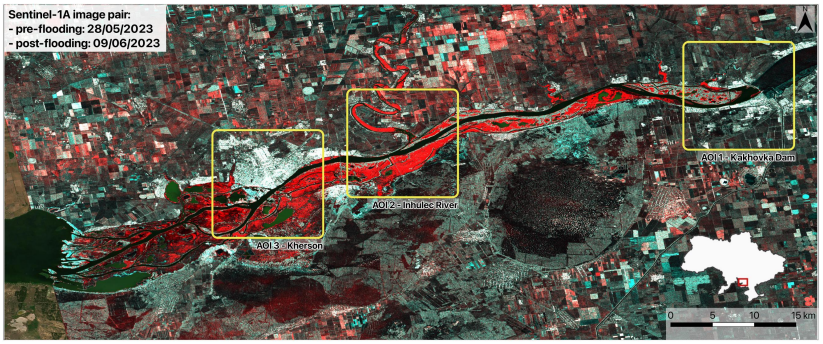

Fig. 5. SAR false-color image depicting in red the flooded areas downstream of the dam, considering the first available date after the dam collapse: June 9th, 2023. In yellow some areas of interest (AOI) are identified

In the context of this flooding analysis scenario, the red color in the imagery shows areas that were submerged by water as a result of the dam collapse. It is worth mentioning that reddish parcels north to the river represent areas that encountered water coverage, either partially or completely, during the second observation epoch. This occurrence is likely attributed to both agricultural activities and/or flooded rivers. The focus is specifically on the downstream area of the dam, as it is the location where the disaster occurred. In this region, significant flooding and water inundation took place. It is important to note that, in contrast to the downstream area, the lake itself experienced a reduction in water level rather than significant flooding.

The first area of interest is, as for the water level scenario, the dam and its surrounding neighborhood. The increase in water level in the Dnieper River following the event led to the submergence of the wetlands just after the Kakhovka dam (Fig. 6a) that were previously visible (Fig. 6b). This situation can be barely seen also in the optical Sentinel-2 image (Fig. 6c) due to the unlucky cloud coverage; in addition to that, the coastline of the lake appeared, indicating the decrease of the water level in the basin due to the collapse of the vertical facing.

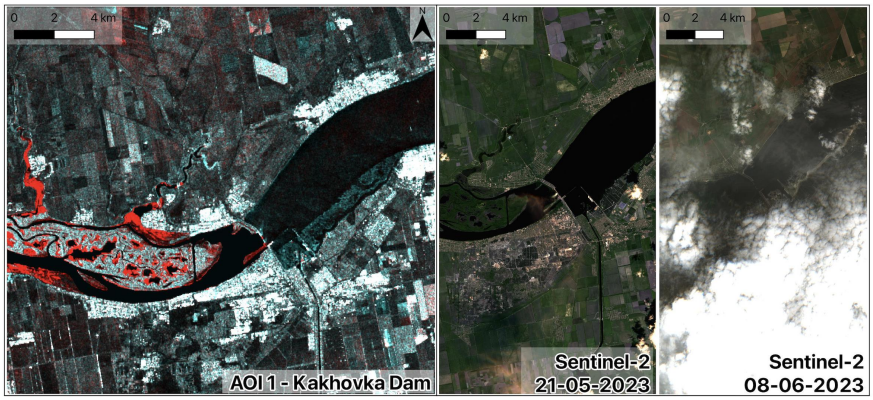

(a) (b) (c)

Fig. 6. Area of interest 1: Kakhovka dam. (a) SAR false-color image; (b) Sentinel-2 optical image, pre-flooding; (c) Sentinel-2 optical image, post-flooding

The second AOI that is considered corresponds to the Inhulec River (Fig. 7), a tributary of the Dnieper River. Here, both the wetlands on the southern bank of the Dnieper and the Inhulec got covered by water. It is very clear from Figure 6a how the small river (black line in the s-shaped riverbed), became several times bigger due to the rise of water, passing

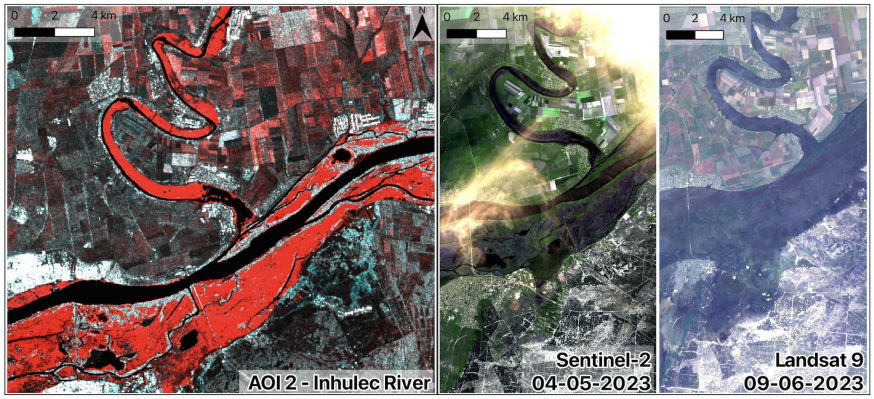

(a) (b) (c)

Fig. 7. Area of interest 2: Inhulec river. (a) SAR false-color image; (b) Sentinel-2 optical image, pre-flooding; (c) Landsat 9 optical image, post-flooding

from about 90 m to about 700 m width. This observation is consistent with the findings from the optical images. Note that the post-event optical image comes from Landsat 9 (U.S. Geological Survey, 2019) as at the revisit time of Sentinel-2 there was too much cloud cover, thus limiting the view.

The third, and final, AOI refers to the city of Kherson and the estuary of the Dnieper River. As shown in Figure 8, the entire southern district of the city was flooded as well as the agricultural fields and wetlands on the southern bank of the Dnieper, as confirmed by the optical images.

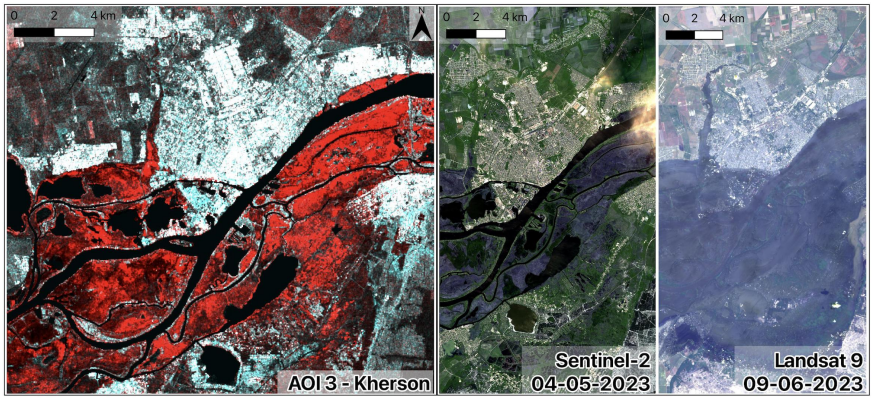

(a) (b) (c)

Fig. 8. Area of interest 3: Kherson. (a) SAR false-color image; (b) Sentinel-2 optical image, pre-flooding; (c) Landsat 9 optical image, post-flooding

4. Discussion

Both the water level and flooding analyses provided valuable insights into the evolving situation surrounding the Nova Kakhovka dam in Ukraine, over the past few months. The usage of the change detection SAR technique enabled the estimation of the areas involved by the variation of the water level in the reservoir and the extent of the flooding that occurred following the collapse of the dam.

Considering water level fluctuations, two distinct classes, "water" and "land", were selected due to their significance. This selection is necessary for the comparative analysis of pre- and post-event classifications, leading to the retrieval of information regarding the extent of the emerged lake shores. Landsat 8 and 9 (U.S. Geological Survey, 2015) multispectral images are the chosen candidates. It is worth mentioning that ESA Sentinel-2 images have partial cloud cover over of the flooded area, making them unsuitable for this numerical validation process. Therefore, for consistency reasons, Landsat products are used also for the water level scenario. The two figures below show the multiband optical images (Fig. 9) and the classified ones (Fig. 10) for the water level variation scenario.

Concerning the flooding event, three distinct classes were designated for the classification process: "water", "buildings/villages", and "fields", encompassing everything not falling into the first two categories. This approach enables the identification and

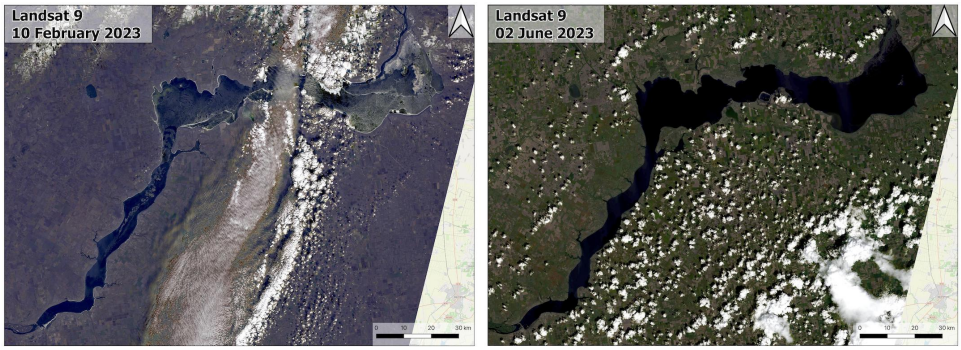

Fig. 9. Landsat 9 optical images for the condition of lowest (left) and highest (right) water level in the reservoir

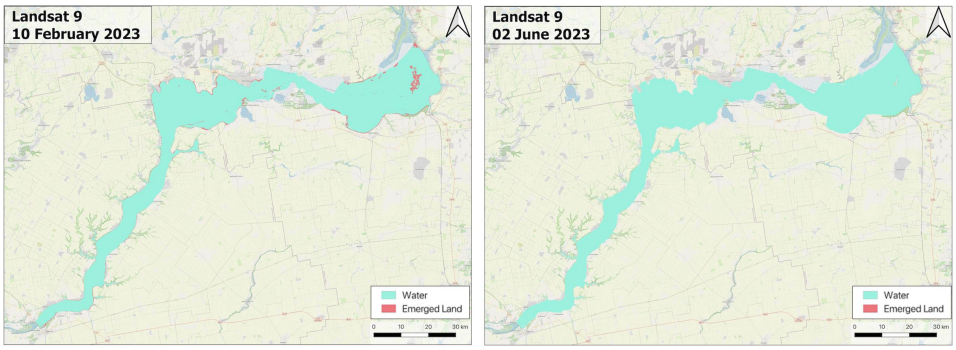

Fig. 10. Landsat 9 classified images for the condition of lowest (left) and highest (right) water level in the reservoir. In red it is shown the emerged lakebed, while in light blue the area of the lake covered by water

quantification of the flood extent while also providing insights into affected human settlements, potentially highlighting areas where people's lives may have been jeopardized. The two figures below show the multiband optical images (Fig. 11) and the classified ones (Fig. 12) for the flooding scenario.

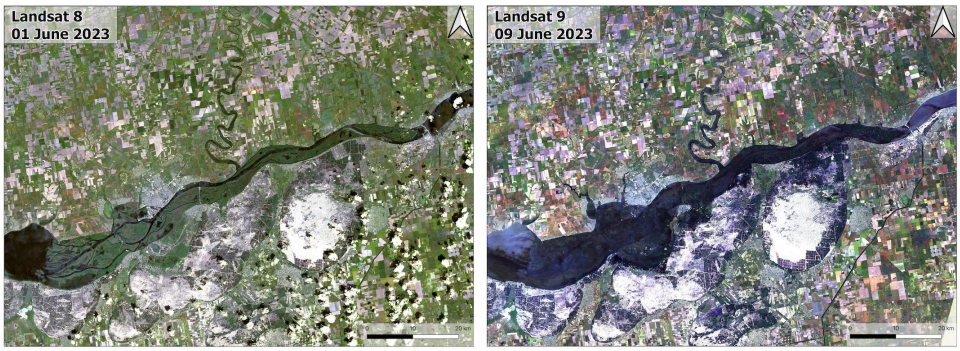

Fig. 11. Landsat 8 and 9 optical images for the pre-flooding (left) and post-flooding (right) condition

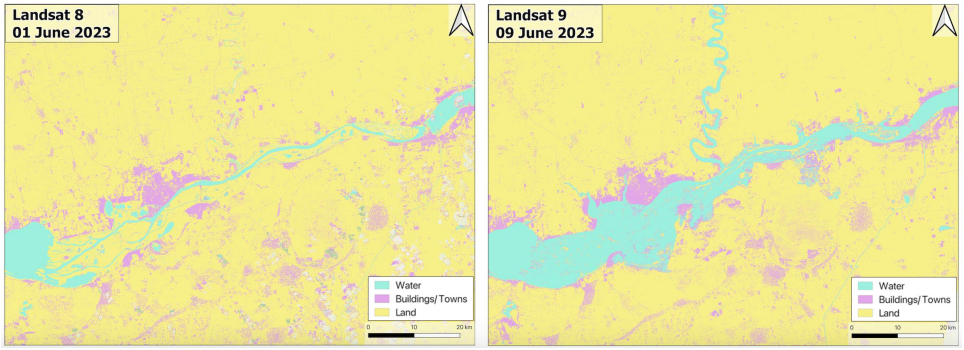

Fig. 12. Landsat 8 and 9 classified images for the pre-flooding (left) and post-flooding (right) condition. In light blue the area of the region covered by water, in pink buildings/villages and in yellow the fields

For both analyzed events, the submerged area due to the water level rise (event one) or flooding (event two) was computed for both SAR and optical sensors; the results are reported in Table 2 (Sentinel-1 images) and Table 3 (Landsat).

Table 2. Submerged areas derived from Sentinel-1 images

Event	Ground resolution (m)	Submerged area (km^2)
Water level change	10×10	45.10
Flooding	30×30	460.00

Table 3. Submerged areas derived from Landsat images

Event	Ground resolution (m)	Submerged area (km^2)
Water level change	30×30	50.00
Flooding	30×30	490.00

The similarity between the two datasets confirmed the reliability of the SAR technique in accurately capturing the effects of water level modifications and the subsequent flooding. The integration of SAR and optical data, along with the validation process, enhances the robustness of the analysis and reinforces the confidence in the findings. The small discrepancies (around 10%), however, are most likely due to the different viewing geometry of the two instrumentations, their different ground resolution, and the results of the pixels' classification.

In the analysis of the water level variation (Fig. 1), in addition to the prominent red coastlines indicating the rise of the reservoir water, there are also large areas that appear in cyan color. These cyan areas can be attributed to a thin layer of snow covering the agricultural fields visible in the February image. This observation suggests that the presence of snow on the fields is causing a distinct reflection intensity variation in the SAR imagery. In fact, cyan is associated to a dominant scattering effect in the first image (February), as it is the result of the combination of green and blue. Furthermore, it is

important to note that within the lake itself, some red pixels emerge from the water body: these red pixels are likely due to residual ice blocks floating over the surface of the basin and it is crucial to not confuse them with emerging lakebed.

The variation in the water level of the lake can also be observed and corroborated through altimetry data (which provides measurements of the height or elevation of the Earth's surface, including bodies of water like lakes) obtained from satellites (i.e., TOPEX, Poseidon, Jason, ERS, ENVISAT, SARAL, Sentinel-3) (USDA Foreign Agricultural Service, 2024). Furthermore, the findings regarding the water level variation were acknowledged and highlighted by the French company Theia, which is specialized in Earth observation and remote sensing applications (Theia, 2023). The time-series of water level variation, obtained from their website, confirms that the detected sudden decrease and subsequent rise of the lake. Figure 13 shows these data, alongside an indication on their accuracy (represented in terms of standard deviation for each epoch by the red bars).

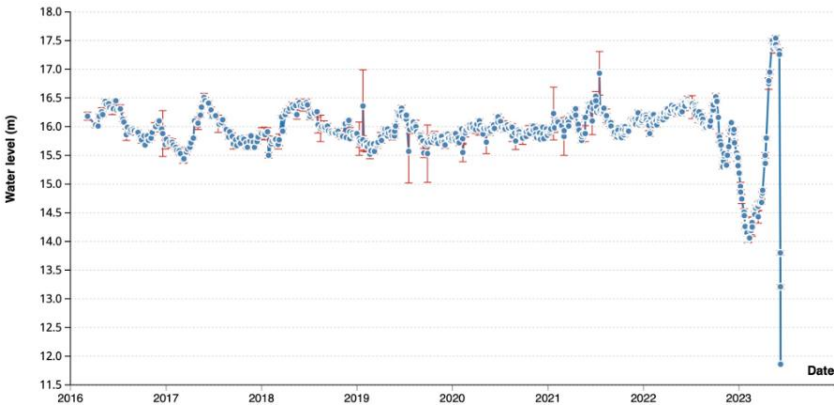

Fig. 13. Water level time series from January 2016 to June 2023 for the Nova Kakhovka Lake, obtained from Theia website. Red bars represent the standard deviation of each observation

On the other hand, regarding the flooding event, it affected an area distributed along almost 80 km, from the Nova Kakhovka dam to the Black Sea. Several newspapers and independent blogs compared the pre- and post-flooding satellite optical images to provide a quick and understandable evaluation of the ongoing disaster. Most of them included Maxar (Maxar Technologies, 2024) high-resolution ground images to assess the damage magnitude and extent. Therefore, they can additionally support and confirm the outcomes of the SAR-based maps presented in this work.

5. Conclusions

The SAR change detection method has proven to be reliable and of quick implementation in case of a variation in the water cover extent, allowing for a fast estimation of the consequences of such events. This is of fundamental importance when assessing damages affecting thousands of people and hundreds of acres of agricultural fields, like it happened

in the case of the Nova Kakhovka dam collapse. It is clear that the increase of the water level in this reservoir dramatically increased the effects of the flooding, as a much larger volume of water (about 7.50 km^3) was released in the Kherson region, submerging everything on its way. Regarding the consistency between SAR and optical data, they differ by 10% in the estimation of the emerged lakebed and by 6% in the estimation of the flooded area. The larger discrepancy for the former estimation is likely due to the geometric distortions of the SAR image's viewing geometry compared to the nadir viewing geometry of the optical image, as well as the different spatial resolutions of the two sensors. Drawing key takeaways from this work, it is evident that fast emergency mapping plays a pivotal role in coordinating first response operations after a disaster. Both optical and radar datasets have proven their capability to accurately estimate the extent of damages. The choice between the two can be based solely on environmental and geometric conditions of the scenario, such as potential cloud cover, and the revisit date of the satellite. This validation underscores the importance of a versatile approach in leveraging the strengths of both optical and radar remote sensing technologies for effective disaster management and response.

Author contributions

Conceptualization: R.M, L.R., M.R.; collection and assembly of data: R.M.; data analysis and interpretation: R.M., L.R.; article writing: R.M.; critical revision and final approval of the article: L.R., M.R.

Data availability statement

Publicly available datasets were analyzed in this study. This data can be found here: https://dataspace.copernicus.eu/.

Acknowledgements

This research received no external funding.

References

Apicella, L., De Martino, M., and Quarati, A. (2022). Copernicus User Uptake: From Data to Applications. *Int. J. Geoinf.*, 11, 121. DOI: 10.3390/ijgi11020121.

Bitek, D., and Erenoğlu, R.C. (2022). Forest Fire Analysis with Sentinel-2 Satellite Imagery: The Case of Mati (Greece) in 2018. *Acad. Platform J. Nat. Hazards and Disaster Managem.*, 3, 85-98. DOI: 10.52114/apjhad.1211651.

Blum, J., Eichhorn, A., Smith, S., et al. (2013). Real-time emergency response: Improved management of real-time information during crisis situations. *J. Multimodal User Interfaces*, 8, 161-173. DOI: 10.1007/s12193-013-0139-7.

Braun, A. (2018). How does multilooking work? Retrieved January, 2024 from https://forum.step.esa.int/t/how-does-multilooking-work/12497/2.

Bullock, J.A., Haddow, G.D., and Coppola, D.P. (2013). *Mitigation, Prevention, and Preparedness*. Introduction to Homeland Security, 435–494. DOI: 10.1016/B978-0-12-415802-3.00010-5.

Columb, M.O., Haji-Michael, P., and Nightingale, P. (2003). Data collection in the emergency setting. *J. Emerg. Med.,* 20, 459–463. DOI: 10.1136/emj.20.5.459.

DeVries, B., Huang, C., Armston, J. et al. (2020). Rapid and robust monitoring of flood events using Sentinel-1 and Landsat data on the Google Earth Engine. *Rem. Sens. Environ.*, 240, 111664. DOI: 10.1016/j.rse.2020.111664.

European Space Agency (2022a). Sentinel-1B in-flight anomaly summary report.

European Space Agency (2022b). Ground Range Detected – Sentinel-1 SAR Technical Guide – Sentinel Online. Retrieved May, 2023 from https://sentinels.copernicus.eu/web/sentinel/technical-guides/sentinel-1-sar/products-algorithms/level-1-algorithms/ground-range-detected.

European Space Agency (2023a). STEP – Science Toolbox Exploitation Platform. Retrieved January, 2024 from https://step.esa.int/main/.

European Space Agency (2023b). Copernicus Data Space Ecosystem / Europe's eyes on Earth. Retrieved January, 2024 from https://dataspace.copernicus.eu/.

European Space Agency and Airbus (2022). Copernicus DEM. DOI: 10.5270/ESA-c5d3d65.

Finnis, A. (2023). Where Nova Kakhovka dam is and what we know about the explosion that breached it. Retrieved January, 2024 from https://inews.co.uk/news/world/nova-kakhovka-dam-where-importance-ukraine-reservoir-blown-up-attack-2389607.

Fletcher, K. (2012). Sentinel-1: ESA's radar observatory mission for GES operational services, ESA SP. ESA Communications, Noordwijk, The Netherlands.

Flores, A., Herndon, K., Thapa, R. et al. (2019). *Synthetic Aperture Radar (SAR) Handbook: Comprehensive Methodologies for Forest Monitoring and Biomass Estimation*. DOI: 10.25966/NR2C-S697.

Gleick, P., Vyshnevskyi, V., and Shevchuk, S. (2023). Rivers and Water Systems as Weapons and Casualties of the Russia-Ukraine War. *Earth's Future*, 11, e2023EF003910. DOI: 10.1029/2023EF003910.

Hoybye, J., Iritz, L., Zheleznyak, M. et al. (2002). Water quality modelling to support the operation of the Kakhovka Reservoir, Dnieper River, Ukraine.

Kecman, V. (2005). *Support Vector Machines – An Introduction, in: Wang, L. (Ed.), Support Vector Machines: Theory and Applications, Studies in Fuzziness and Soft Computing*. Springer, Berlin, Heidelberg, pp. 1–47. DOI: 10.1007/10984697_1.

Knight, M. (2023). Kakhovka dam collapse has made Black Sea a "garbage dump and animal cemetery," Ukraine warns. Retrieved June, 2023 from https://edition.cnn.com/2023/06/11/europe/kakhovka-dam-collapse-swimming-banned-intl-hnk/index.html.

Kottasova, I., and Mezzofiore, G. (2023). Nova Kakhovka dam: Here are the key theories on what caused Ukraine's catastrophic dam collapse |CNN. Retrieved June, 2023 from https://edition.cnn.com/2023/06/08/europe/nova-kakhovka-destruction-theories-intl/index.html.

Krichen, M., Abdalzaher, M.S., Elwekeil, M., et al. (2024). Managing natural disasters: An analysis of technological advancements, opportunities, and challenges. *Internet of Things and Cyber-Physical Systems*, 4, 99–109. DOI: 10.1016/j.iotcps.2023.09.002.

Kuzova, N., (2023). The Tragedy of Kakhovka Reservoir. Retrieved January, 2024 from https://www.iwm.at/blog/the-tragedy-of-kakhovka-reservoir.

Malmgren-Hansen, D., Sohnesen, T., Fisker, P. et al. (2020). Sentinel-1 Change Detection Analysis for Cyclone Damage Assessment in Urban Environments. *Rem. Sens.*, 12, 2409. DOI: 10.3390/rs12152409.

Mansourpour, M., and Blais, R. (2006). Effects and performance of speckle noise reduction filters on active radar and SAR images. *Proc. ISPRS*, 36, W41.

Mateo-Garcia, G., Veitch-Michaelis, J., Smith, L. et al. (2021). Towards global flood mapping onboard low cost satellites with machine learning. *Sci. Rep.* 11, 7249. DOI: 10.1038/s41598-021-86650-z.

Maxar Technologies (2024). Earth Intelligence & Space Infrastructure. Retrieved June, 2023 from https://www.maxar.com/.

Mitraka, Z., Siachalou, S., Doxani, G. et al. (2020). Decision Support on Monitoring and Disaster Management in Agriculture with Copernicus Sentinel Applications. *Sustainability*, 12, 1–20. DOI: 10.3390/su12031233.

Nasirzadehdizaji, R., Akyuz, D.E., and Cakir, Z. (2019). Flood mapping and permanent water bodies change detection using sentinel SAR data. The International Archives of the Photogrammetry. *Rem. Sens. Spatial Inf. Sci.*, XLII-4-W18, 797–801. DOI: 10.5194/isprs-archives-XLII-4-W18-797-2019.

Reguzzoni, M., Rossi, L., De Gaetani, C.I., et al. (2022). GNSS-Based Dam Monitoring: The Application of a Statistical Approach for Time Series Analysis to a Case Study. *Appl. Sci.*, 12, 9981. DOI: 10.3390/app12199981.

Rignot, E.J.M., and van Zyl, J.J. (1993). Change detection techniques for ERS-1 SAR data. *IEEE Trans. Geosci. Rem. Sens.*, 31, 896–906. DOI: 10.1109/36.239913.

Santoso, A.W., Bayuaji, L., Pebrianti, D. et al. (2016). A fuzzy approach for speckle noise reduction in SAR images. *Int. J. Adv. Appl. Sci.*, 3(5), 33–38.

Skarpa, P.E., Simoglou, K.B., and Garoufallou, E. (2023). Russo-Ukrainian War and Trust or Mistrust in Information: A Snapshot of Individuals' Perceptions in Greece. *Journalism and Media*, 4, 835–852. DOI: 10.3390/journalmedia4030052.

Smith, P., and Butterworth, M. (2023). Satellite images show the scale of the Ukraine dam destruction. Retrieved January, 2024 from https://www.nbcnews.com/news/world/satellite-images-show-ukraine-dam-destruction-rcna88299.

Stelmaszczuk-Gorska, M. (2020). Flood mapping with synthetic aperture radar. EO4GEO. Retrieved June, 2023 from http://www.eo4geo.eu/training/flood-mapping-with-synthetic-aperture-radar/.

Tarpanelli, A., Mondini, A.C., and Camici, S. (2022). Effectiveness of Sentinel-1 and Sentinel-2 for flood detection assessment in Europe. *Nat. Hazards Earth Sys. Sci.*, 22, 2473–2489. DOI: 10.5194/nhess-22-2473-2022.

Tay, C.W.J., Yun, S.-H., Chin, S.T. et al. (2020). Rapid flood and damage mapping using synthetic aperture radar in response to Typhoon Hagibis. *Japan. Sci. Data*, 7, 100. DOI: 10.1038/s41597-020-0443-5.

Theia (2023). What Hydroweb data shows about the Kakhovka dam failure – Theia. Retrieved June, 2023 from https://www.theia-land.fr/en/what-hydroweb-data-shows-about-the-kakhovka-dam-failure/.

Torres, R., Snoeij, P., Geudtner, D. et al. (2012). GMES Sentinel-1 mission. *Rem. Sens. Environ.*, 120, 9–24. DOI: 10.1016/j.rse.2011.05.028.

U.S. Geological Survey (2015). Landsat – Earth observation satellites (No. 2015–3081), Fact Sheet. U.S. Geological Survey. DOI: 10.3133/fs20153081.

U.S. Geological Survey (2019). Landsat 9 (No. 2019–3008), Fact Sheet. U.S. Geological Survey. DOI: 10.3133/fs20193008.

USDA Foreign Agricultural Service (2023). Water level in the Kakhovka Reservoir in Ukraine from January 6, 2020 to September 6, 2023, by satellite Retrieved January, 2024 from https://www.statista.com/statistics/1391641/kakhovka-reservoir-water-level/.

USDA Foreign Agricultural Service (2024). G-REALM – Kakhovskoye. Retrieved June, 2023 from https://ipad.fas.usda.gov/cropexplorer/global_reservoir/gr_regional_chart.aspx?regionid$=$up{&}reservoir_name$=$Kakhovskoye{&}lakeid$=$000873.

Vavassori, A., Carrion, D., Zaragozi, B. et al. (2022). VGI and Satellite Imagery Integration for Crisis Mapping of Flood Events. *ISPRS Int. J. Geoinf.*, 11, 611. DOI: 10.3390/ijgi11120611.

Vavriv, D.M., and Bezvesilniy, O.O. (2013). Advantages of multi-look SAR processing, in: 2013 IX Internatioal Conference on Antenna Theory and Techniques. In the 2013 IX International Conference on Antenna Theory and Techniques, pp. 217–219, September, 16–20, Odessa, Ukraine. DOI: 10.1109/ICATT.2013.6650730.

Vincent, R.K. (2003). *RADAR / Synthetic Aperture Radar (Land Surface Applications)*. In Holton, J.R. (Ed.), Encyclopedia of Atmospheric Sciences. Academic Press, Oxford, pp. 1851–1859. DOI: 10.1016/B0-12-227090-8/00331-6.

Vyshnevskyi, V., Shevchuk, S., Komorin, V. et al. (2023). The destruction of the Kakhovka dam and its consequences. *Water Int.*, 48, 631–647. DOI: 10.1080/02508060.2023.2247679.

Yerushalmy, J. (2023). Nova Kakhovka dam: everything you need to know about Ukraine's strategically important reservoir. The Guardian.

Yu, Z., Wang, W., Li, C. et al. (2018). Speckle Noise Suppression in SAR Images Using a Three-Step Algorithm. *Sensors*, 18, 3643. DOI: 10.3390/s18113643.